X-RAY IN-SITU SATURATION IN GAS CONDENSATE RELATIVE PERMEABILTY STUDIES

Andrew Cable, Robert Mott, Mike Spearing (AEA Technology plc)

ABSTRACT

Well productivity in gas condensate reservoirs is often reduced by condensate banking when the well bottom hole pressure falls below the dew point pressure. The most important parameter for determining condensate well productivity is the effective gas permeability in the near-well region. A number of laboratory experiments have been undertaken using x-ray in-situ saturation monitoring to measure condensate saturation at steady-state conditions during high rate (near-well) core flooding.

This paper presents results from x-ray in-situ saturation monitoring for six near-well experiments on a low permeability (12md) core at high-velocities. Measurements were undertaken at a range of interfacial tensions and velocities to distinguish between high capillary number and inertial flow effects. Measured condensate saturations were in the range of 20%-50% depending upon the richness (composition) of the gas condensate fluid used and the gas flow rate. Interestingly, the measured condensate saturation was found to increase with flow rate. Our results show that the improved gas mobility at high capillary number is not due to lower condensate saturation. (The widely used term "velocity stripping" gives a misleading impression of the phenomena which take place in the near-well region). The condensate saturation distribution was found to be uniform; there was no evidence of condensate banking, end effects or desaturation effects. The measured in-situ saturation measurements were found to be consistent with modelled condensate saturation.

1. INTRODUCTION

Results are given from high rate relative permeability and inertial flow coefficient measurements on Obernkirchner outcrop sandstone core. This core has low permeability (absolute gas permeability of 12 md) and high porosity (20%). The experiments used a 5-component synthetic condensate fluid, at a temperature of 60^{o}C. At this temperature the measured dew point pressure was 212 bar.

Experiments were carried out above the dew point pressure to measure the inertial (non-Darcy) flow coefficient, and below the dew point pressure to measure the gas and oil relative permeability. We refer to these experiments as single-phase and two-phase respectively, according to the number of hydrocarbon phases which were present. An initial water saturation of about 5% was present in the core during these experiments. In-situ saturation data were obtained using x-ray attenuation at steady state flowing conditions.

2. EXPERIMENTAL EQUIPMENT

The near-well bore flow circuit is designed to undertake high rate flow experiments to measure steady-state gas relative permeability k_{rg} as a function of k_{rg}/k_{ro}. (The ratio k_{rg}/k_{ro} may be thought of as a measure of the fractional flow of the gas and oil phases in the near-well region). The circuit is housed in an oven and custom-built to allow the use of x-ray in-situ saturation monitoring. The set up is shown in Figures 1 and 2. The maximum operating temperature is 80°C and core confining pressures of up to 275 bar (4,000 psi) may be used. These constraints, and hence the use of a synthetic gas condensate, were imposed by the use of a low x-ray attenuating aluminium core holder (used to contain the core material in a vertical orientation). A full description of the equipment and the operating procedures are presented in reference [1].

The facility is shown schematically in Figure 2 and comprises a rigid gantry assembly which supports the vertical translational system of x-ray tube and detector. The rig is mounted on a 3.8 m long platform which can be positioned to within 100 μm relative to the x-ray/detector system. The x-ray scanner enables high resolution saturation information to be generated and has the capability to operate in both single and dual energy modes (allowing 2-phase and/or 3-phase data to be collected). The computer-controlled x-ray system is fully automated and provides a high photon flux, high stability and low ripple x-ray generation. The line array detector system allows a 0.5 mm resolution over a 512 mm field of view using 1024 detector elements. The detector shows excellent repeatability (within 0.02%), which is essential for core flood studies. The detector head can be rotated by 90° allowing horizontal or vertical measurements. For the high rate core floods, the detector was set up in a vertical orientation to minimise scanning time. The complete length of the core was scanned in one exposure and four 6.4 mm wide vertical lines were used to cover approximately 80% of the pore space.

The x-ray beam is subject to long term drift, short term ripple and fluctuations on the individual detector elements. To overcome this drift, the raw x-ray data are normalised. Two forms of normalisation are used to monitor the small detector changes over the duration of the study, which sometimes may last many months. (1) **Edge Reference**: An aluminium reference (of equal attenuation to the core/coreholder system) is taken at the same time as each core measurement, for each line of data. (2) **White Reference**: At the start of a core scan sequence, a measurement is made on an aluminium reference covering the full 512 mm field of view. This reference is compared back to the initial measurement made at the start of the test to give a normalisation factor for each detector element.

The statistical accuracy demanded from the x-ray scanner depends upon whether 2-phase or 3-phase data are required and the in-situ fluid saturation accuracy required. In practice, the saturation accuracy is constrained by three factors: (a) The difference in linear attenuation coefficient of the fluids, which depends mainly on the densities of the fluids. With condensate systems, the density difference between liquid and gas phases is inherently small, which leads to either long scan times or poor saturation accuracies.

(b) Time limitations, whether a scan is required during a dynamic flood or at steady-state conditions. (c) The desired spatial resolution of the data.

The above factors have to be taken into account when defining a scanning program for a core flood study. The factors are optimised to obtain good in-situ saturation accuracy in a practical time frame. At reservoir conditions, oven walls and high pressure core holders dictate high x-ray energies just to penetrate the target and longer x-ray scan times to achieve a given count. At these high energies, the fluids are less attenuating and saturation accuracy is reduced still further. All these issues contribute to the complexities of producing accurate saturation measurements on condensate systems.

For the near-well bore tests, dopant was **not** used to improve saturation accuracy, to avoid unpredictable fluid behaviour and extra PVT modelling on the 5-component fluid. The saturation accuracy for the near-well bore test was estimated using spreadsheet tools that allow the factors mentioned above to be modelled for both 2-phase and 3-phase tests [2]. The predicted saturation error for 3-phase tests on a condensate system was up to 16% PV compared to less than 2.5% PV for the 2-phase case (assuming an immobile water saturation).

The polychromatic nature of x-rays leads to a hardening of the x-ray beam on penetration of a material, where the lower energy parts of the spectrum are preferentially absorbed. This so called 'beam hardening' is an additional factor which affects the measured saturation. A suite of software codes has been developed to model the beam hardening process. The effect depends on many factors, in particular the concentration of dopant, type of dopant and fluid thickness (core diameter and porosity). In the 2-phase near-well bore test (using a 0.56 mm copper filter to pre-harden the beam) the effect of beam hardening on the saturation was been found to be negligible.

3. CORE MATERIAL AND GAS CONDENSATE FLUID

For this study an outcrop sandstone was used (Obernkirchner). The core was initially CT scanned to ensure that the sample was homogeneous. The core was prepared with an initial water saturation (S_{wi}) of 0.053 PV, measured using a γ-ray in-situ hydrocarbon dispersion technique. Core properties are given in Table 1:

TABLE 1 – CORE CHARACTERISATION DATA

Description	Obernkirchner Outcrop Core
Mean Length (cm)	28.60
Mean Diameter (cm)	3.79
Pore Volume (cm^3)	64.50
Porosity (%)	20.0
Abs Gas Permeability (md)	12.0
S_{wi} (PV)	0.053
K_e – Reference (md)	7.7

The fluid used was a 5-component synthetic gas condensate. The composition of this fluid and the predicted and measured liquid dropout characteristics are given in reference [1]. For the test temperature at 60°C, the measured dew point pressure was 212 bar.

4 RESULTS FROM NEAR-WELL BORE EXPERIMENT

Two sets of measurements were carried out with the core inlet pressure at 230 and 250 bar, well above the fluid dew point pressure of 212 bar. The results were used to calculate permeability and estimate the inertial (non-Darcy) flow coefficient using the analysis of Evans et al [3]. Figure 3 shows a plot of mass flow rate versus ΔP^2 (the permeability and inertial flow coefficient can also be estimated from this plot). Due to the low permeability of the core and the high flow rates used, some of the experiments involved a pressure drop across the core in excess of 30 bar. The analysis methods were therefore modified to allow for the variation in gas viscosity and Z-factor along the core length. The analyses gave absolute permeabilities between 8.4 and 8.7 md, and inertial flow coefficients between 0.30 and 0.34 x 10^{-10} m^{-1}. There was a significant inertial flow effect at the higher rates in these experiments; the straight line in Figure 3 shows the results expected for Darcy flow if there were no inertial effects present.

Five two-phase experiments were carried out at different core inlet pressures and flowing fluid compositions. In each series of measurements, the core inlet pressure and flowing fluid composition were fixed while the core outlet pressure was changed to vary the flow rate. The core conditions are representative of the near-well region and the flowing fluid represents the gas phase flowing into the near-well region from the main part of the reservoir. The flowing fluid is defined in terms of its saturation pressure. The measurements are summarised in Table 2.

TABLE 2 – CONDITIONS FOR TWO PHASE EXPERIMENTS

High Rate Experiment	Saturation pressure of fluid (bar)	Flash across inlet valve (bar)	Core inlet pressure (bar)	Core outlet pressure (bar)
hr_190	190	10	180	168 – 179
hr_170	170	10	160	140 – 159
hr_140	140	10	130	96 – 130
hr_200	200	20	180	161 – 179
hr_150	150	20	130	95 – 129

The pressure drop across the core was measured, together with the volumetric flow rates of the oil and gas phases at the core outlet pressure. When the pressure drop across the core was large, the volumetric flow rates varied along the length of the core, especially for the oil phase since liquid condensation is occurring along the length of the core. (This is illustrated in Figure 11). However, at steady state conditions, the phase flow rates will be proportional to the phase volumes in a Constant Composition Expansion (CCE) on the flowing fluid composition. If the oil flow rate Q_o at the outlet pressure P_{out} is known, it is possible to estimate the oil phase flow rate at any pressure from:

$$\frac{Q_o(P)}{Q_o(P_{out})} = \frac{V_o(P)}{V_o(P_{out})}$$

where the CCE volumes V_o can be calculated from an Equation of State (EoS) model of the synthetic condensate. A similar expression can be used to estimate the gas flow rate. PVT properties such as viscosity and IFT will also vary along the core, but they can be again predicted from the EoS model. These methods were used to convert the flow rates measured at the core outlet pressure to flow rates at the mean core pressure. The effective permeabilities were then calculated using flow rates and viscosities at the mean core pressure. Capillary number was also calculated at the mean core pressure.

It is possible to predict the steady state ratio of k_{rg}/k_{ro} from the fluid PVT properties, using the EoS model. The measured data are compared with the predicted values in Figure 4. The pressure on the x-axis is the mean core pressure (defined as the average of the inlet and outlet pressures), and the measured data were calculated from the flow rates at the mean core pressures. There is reasonable agreement between the measured and predicted data, except for a few points. The most obvious discrepancies are at the right hand end of the set for each experiment. These points correspond to the lowest flow rates and are subject to greater experimental error due to the small pressure drop (about 1 bar).

Figure 5 shows the measured gas and oil (condensate) relative permeabilities, plotted as a function of capillary number, for each of the five experiments. The data show a clear trend of increasing gas relative permeability with capillary number, and there is also some evidence for the oil relative permeability increasing with capillary number, especially when capillary number is above about 10^{-4}. The higher oil relative permeabilities for experiment hr_200 are due to the richer gas condensate giving higher oil saturations in the core.

Three of the experiments (hr_190, hr_170 and hr_150) were carried out at similar values of the k_{rg}/k_{ro} ratio, but at different pressures, and hence different IFT's. The conditions for these three experiments are summarised in Table 3. As capillary number is proportional to (velocity / IFT), the velocity to achieve a given capillary number is proportional to the IFT. Thus the velocities at a given capillary number are highest in experiment hr_150, next highest in hr_170, and lowest in hr_190.

TABLE 3. EXPERIMENTS HR_190, HR_170, AND HR_150

Name	Mean core pressure (bar a)	IFT at P_{mean} (mN/m)	Superficial velocities (m/day)
hr_190	175 - 181	0.2 – 0.25	16 – 300
hr_170	151 - 161	0.4 – 0.6	18 - 500
hr_150	114 - 131	1.2 – 1.9	23 - 850

The results in Figure 5 show that for a fixed capillary number and k_{rg}/k_{ro} ratio, gas relative permeability decreases with increasing velocity, whereas most models for gas

condensate relative permeability have been based on the assumption that high-velocity effects can be correlated as a function of the capillary number alone [4]. These results do not fit into such a model. The gas relative permeabilities in Figure 5 include the competing effects of both inertial flow and high capillary number flow, which explains why they cannot be modelled as a function of capillary number alone. The higher velocities for hr_150 would lead to a larger inertial effect, so reducing the effective gas permeability.

Interpretation of these experimental results can be simplified if the inertial and high capillary number flow effects are modelled separately. Inertial flow effects are represented by a separate multiplication factor (based on the measured single-phase inertial flow coefficient) and so excluded from the relative permeability. With this alternative definition of relative permeability, the gas relative permeability in these experiments can be modelled as a function of capillary number alone, and the data fitted to existing correlations. A detailed discussion of the modelling of the experimental results is given in reference [5].

5 RESULTS FROM IN-SITU SATURATION MONITORING

Single energy, two-phase x-ray scanning was performed throughout the study, making the assumption that below the dew point pressure the third-phase was immobile brine. To check the brine saturation during the study, x-ray scans were performed each time the core was re-saturated with single phase condensate above the dew point pressure. Two calibration scans were required with the available pore volume fully saturated with each of the two phases present i.e. 100% PV single phase gas condensate and 100% PV brine. These calibrations were undertaken at the end of the 10 month study since reservoir condition, miscible solvent flooding was required to remove the irreducible brine phase, S_{wi}. By referencing the scan data to the calibrations, a measurement of S_{wi} prior to each experiment was achieved.

The brine saturation measured before the study using independent γ-ray techniques was 0.053 PV, which compared to an initial x-ray in-situ saturation measurement of 0.064 PV using nitrogen scans at the test conditions of 230 bar at 60°C (100% nitrogen and brine calibrations also performed at the end of the study). Brine saturations derived from the single phase gas condensate scans are presented in Table 4 and Figure 6.

TABLE 4 – X-ray S_{wi} SCANS UNDERTAKEN THROUGHOUT STUDY

High rate experiment	No. of weeks	In-situ S_{wi}
1. Single phase condensate introduced	0	0.072
2. Following 1-ϕ measurements, hr_250 & hr_230	3	0.050
3. Following hr_190, hr_170 & hr_140 test sequence	10	0.060
4. Following hr_200 and hr_150 test sequence	20	0.018
5. Following extended high rate test hr_150	26	0.025

For the two-phase gas condensate tests below the dew point pressure, calibrations were required for 100% HCPV equilibrium gas (at S_{wi}) at each test pressure and likewise 100% HCPV equilibrium condensate (at S_{wi}) at each test pressure. The equilibrium gas calibrations at S_{wi} were performed at the end of each test sequence (given in Table 4) so that calibrations were true, given the small observed decreases in S_{wi}. The equilibrium oil calibrations at S_{wi} for all experiments were performed at the end of the last test, so here the calibrations were only true for hr_200 and hr_150. A condensate saturation error of around –1% HCPV for experiment hr_140 and –2% HCPV for hr_190 was estimated given the decrease in S_{wi} of around 0.030 PV observed since the time that the x-ray scan was taken.

For each high rate experiment, x-ray scanning was carried out during two different flow rates. Most of the measurements were carried out at relatively low flow rates, primarily so that not too much fluid was spent during the x-ray scan that lasted approximately one hour. The average values for saturation are shown in Table 5. Saturation profiles for the high rate floods are shown in Figures 7 to 11.

TABLE 5 – TWO-PHASE, X-RAY IN-SITU SATURATION RESULTS

High rate experiment	Flow rate L/h	K_{rg}/k_{ro}	Capillary number	Condensate saturation, % HCPV
hr_190	0.15	7.9	2.3E-05	28
	0.58	9.9	9.0E-05	32
hr_170	0.17	17.1	1.1E-05	30
	0.46	18.6	3.1E-05	29
hr_140	0.25	162	4.7E-06	22
	0.53	54.2	9.5E-06	28
hr_200	0.21	4.1	3.1E-05	48
	0.72	3.6	1.0E-04	52
hr_150	0.21	12.1	3.8E-06	40
	0.54	16.6	9.5E-06	44
hr_150	0.20	12.1	3.8E-06	29
(extended test)	7.5	14.2	8.3E-05	40

The ratio k_{rg}/k_{ro} presented in Figure 4 may be thought of as a measure of the fractional flow of the gas and oil phases and as the ratio k_{rg}/k_{ro} decreases, the condensate saturation

increases. The predicted and measured data plots presented in Figure 4 are grouped for each experiment (with decreasing k_{rg}/k_{ro} ratio) and the first two points on the right hand side of each data set (except hr_150 extended test) correspond to the in-situ data. It is apparent from Table 5 that all condensate saturations lie within an approximate range of 20% to 50% HCPV, with the condensate saturation increasing with capillary number. The condensate saturation for test hr_200 is notably higher, and generally for the test hr_190 the condensate saturation is higher than that of hr_170 which is higher than hr_140. The repeated low rate data for hr_150 is similar to hr_170. These saturations are consistent given the changes (or similarities) in k_{rg}/k_{ro} ratio for each experiment. The saturation distributions are uniform along the core with no evidence for condensate banking, capillary end effect or desaturation effects. There is an "entrance effect" covering the first 3 to 4 cm of the core on most scans, which may be attributed to the establishment of stabilised flow following the fluid flash through the pressure reducing valve. Although the entrance effects observed are not fully understood, the fact that it was identified adds credence to the observations that no outlet effects were evident.

The test hr_150 was repeated to obtain data at a very high flow rate. There was an inconsistency between the two sets of results for hr_150 at the low flow rate. (Without further measurement, the reason for this is not clear). For all but the last experiment, the flow rates are relatively low with the pressure drop across the core being of the order of 1 bar. For the last experiment (hr_150 at 7.5 L/hr), the pressure drop was about 35 bar. To quantify the saturation of this test, the calibration scans were extrapolated to the 95 bar outlet pressure and it was necessary to assume a linear pressure decline across the core to obtain incremental calibrations as a function of pressure. The resulting saturation profile is given in Figure 11 and the condensate saturation increases along the core from about 35% at the inlet to 45% at the outlet.

The results in Table 5 show that, in most cases, condensate saturation increases with higher capillary number at a constant value of the k_{rg}/k_{ro} ratio. This is consistent with the general trend of experimental results given in Figure 5, which show a much larger increase in gas permeability than in condensate permeability at high capillary number. It appears that the improved gas mobility at high capillary number is not due to lower condensate saturation. This may be surprising as the term 'velocity stripping' implies that the improvement in well productivity due to capillary number effects is due to reduced condensate saturations in the near-well region.

7. DISCUSSION AND CONCLUSIONS

It is clear from our results presented in Figure 5, that the gas relative permeability increases with capillary number. For instance test hr_190, where gas relative permeability increases from about 0.2 to 0.4 for a capillary number increase of around $2x10^{-5}$ to $3x10^{-4}$. There is also an increase in the condensate relative permeability from around 0.02 to 0.05.

However, from Figure 4, tests hr_190, hr_170 and hr_150 can be seen to be conducted at an approximately constant k_{rg}/k_{ro} ratio of 10. Figure 5 shows therefore, that for a fixed

capillary number (and k_{rg}/k_{ro} ratio of 10), the gas relative permeability decreases. Remembering that IFT is higher at the lower test pressure for test hr_150 and also that the gas velocity is proportional to capillary number and IFT, for a constant capillary number, the gas velocity is highest for test hr_150 (and lowest for hr_190). Gas relative permeability is therefore shown to decrease with an increased gas velocity.

These experiments show two effects; an increase in both gas and condensate relative permeability due to high capillary number flow, and a reduction in effective gas permeability at high gas velocities due to inertial flow. For this reason, models for gas condensate relative permeability should not be correlated as a function of the capillary number alone. For the core, fluid system and flow rates we used, the capillary number effect is more dominant, so that the combined effect is to increase both gas and condensate mobility. The changes in relative permeability at high capillary number can lead to significant increases in calculated well productivity [5].

The test procedures developed to enable x-ray in-situ saturation monitoring to be used for these near-well bore flow experiments were very successful. A number of x-ray scans were undertaken which have been presented in this paper. The condensate saturation distributions were found to be uniform for the rates measured (up to 0.6L/h) and there was little evidence for condensate banking, capillary end effects or desaturation effects in the core outlet region. For the test at 7.5 L/h, the pressure drop was around 35 bar and the condensate saturation was observed to increase from 35% at the inlet to 45% at the outlet for the core length of 28 cm.

The measured condensate saturation increases with higher capillary number at a constant value of the k_{rg}/k_{ro} ratio. This may be surprising as the term “velocity stripping” implies that the improvement in well productivity at high capillary number is due to reduced condensate saturation. However, the increased condensate saturation is consistent with the fact that high capillary numbers lead to a much larger increase in gas permeability than in condensate permeability.

To illustrate this point, Figure 12 shows gas and oil relative permeability curves at low and high capillary numbers. To examine the data at a fixed value of the k_{rg}/k_{ro} ratio, it is easiest to consider a k_{rg}/k_{ro} ratio of 1, the point where the gas and oil curves cross. An increase in capillary number moves this crossover point from A to B on Figure 12, leading to a higher condensate saturation as well as increasing both gas and oil relative permeabilities.

Our measurements have shown that the improved gas mobility at high capillary number is not due to lower condensate saturation. The widely used term “velocity stripping” gives a misleading impression of the phenomena which actually take place in the near-well region.

ACKNOWLEDGEMENTS

The authors wish to express their gratitude and acknowledge the financial support for this project from the U.K. Department of Trade & Industry, European Commission, BP-Amoco, Esso UK E&P, Marathon Oil UK Ltd, Mobil North Sea, Phillips Petroleum Company UK Ltd, SAGA Petroleum a.s. and Texaco Britain Limited.

REFERENCES

1 Cable A S, Mott R E, and Spearing M C "Experimental Techniques for the Measurement of Relative Permeability and In-Situ Saturation in Gas Condensate Near-Well Bore and Drainage Studies" SCA-9928, Society of Core Analysts Symposium, Golden, Colorado, August 1999.

2 Naylor, P., Puckett, D. A. 'In-Situ Saturation Distributions: The Key to Understanding Core Analysis', SCA-9405, presented at Society of Core Analysts Symposium, Stavanger, September 1994.

3 R.D.Evans et al, 'The Effect of an Immobile Liquid Saturation on the Non-Darcy Flow Coefficient in Porous Media', SPE Prod Eng, November 1987.

4 S.M.P.Blom and J.Hagoort 'How to Include the Capillary Number in Gas Condensate Relative Permeability Functions?' SPE 49268, SPE Annual Technical Conference and Exhibition, New Orleans, September 1998.

5 Mott R E, Cable A S, and Spearing M C "Measurement and Simulation of Inertial and High Capillary Number Flow Phenomena in Gas-Condensate Relative Permeability" SPE 62932, SPE Annual Technical Conference and Exhibition, Dallas, Texas, 1-4 October 2000.

FIGURE 1: Schematic Diagram Condensate Module Flow Circuit

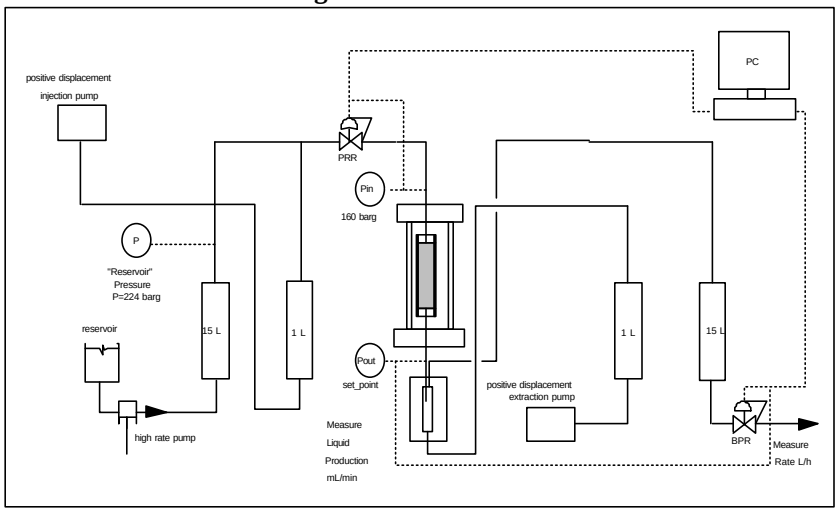

FIGURE 2: Schematic diagram of the x-ray scanner

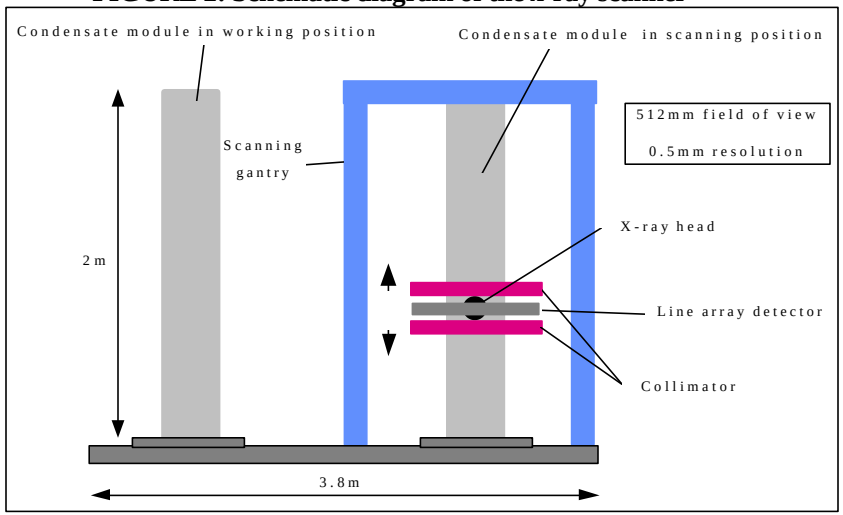

FIGURE 3: DP^2 versus flow rate, single phase test

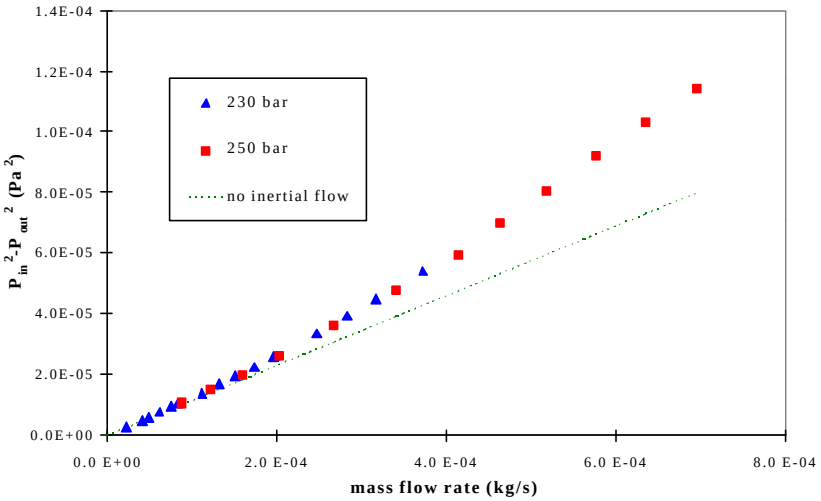

FIGURE 4: Predicted and measured *krg/kro*

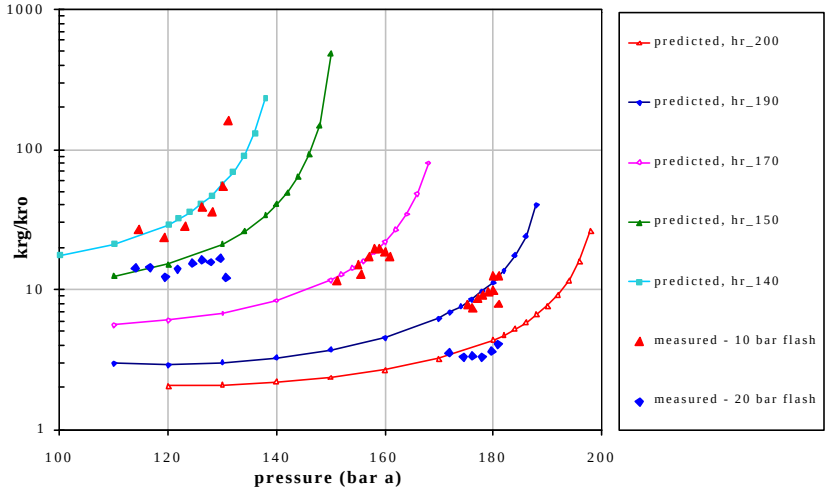

FIGURE 5: Relative permeability versus capillary number

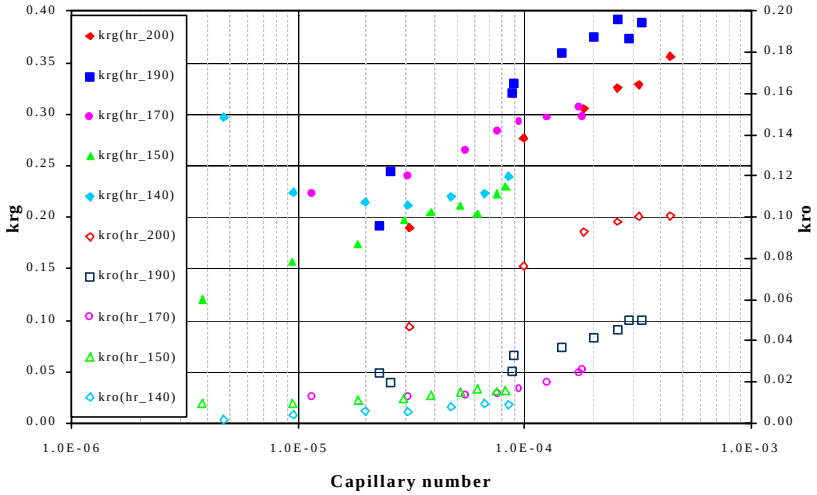

FIGURE 6: Brine saturation profiles during study

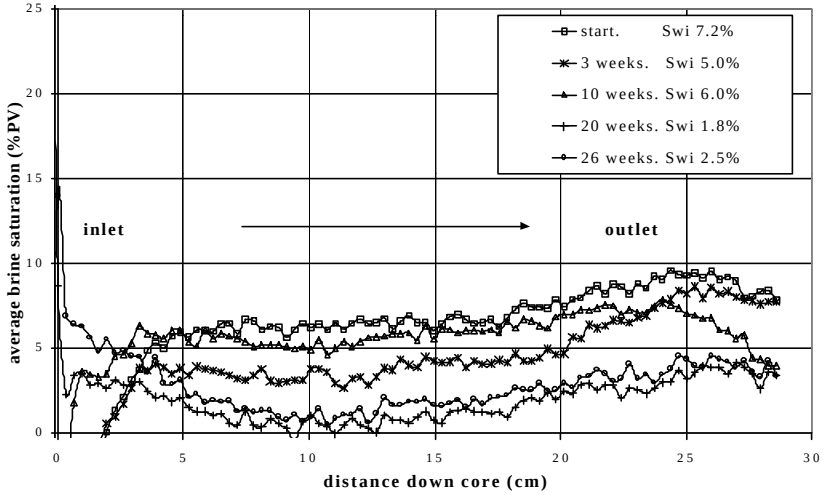

FIGURE 7: Condensate saturation profile test hr_190

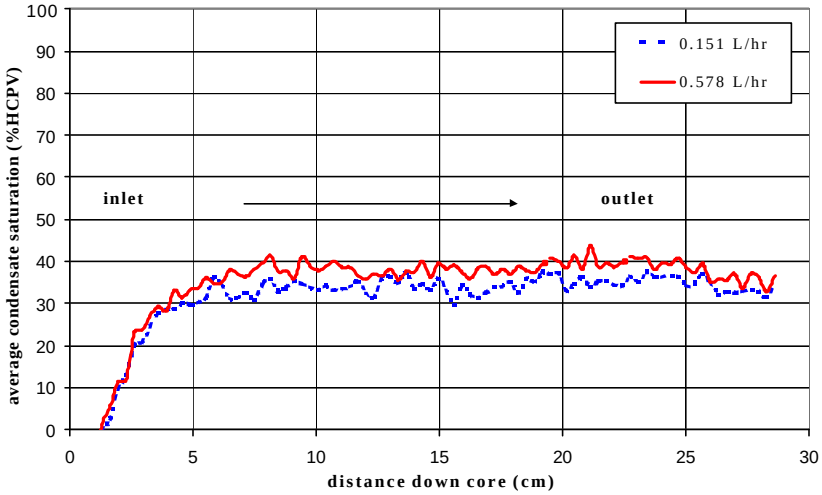

FIGURE 8: Condensate saturation profile test hr_170

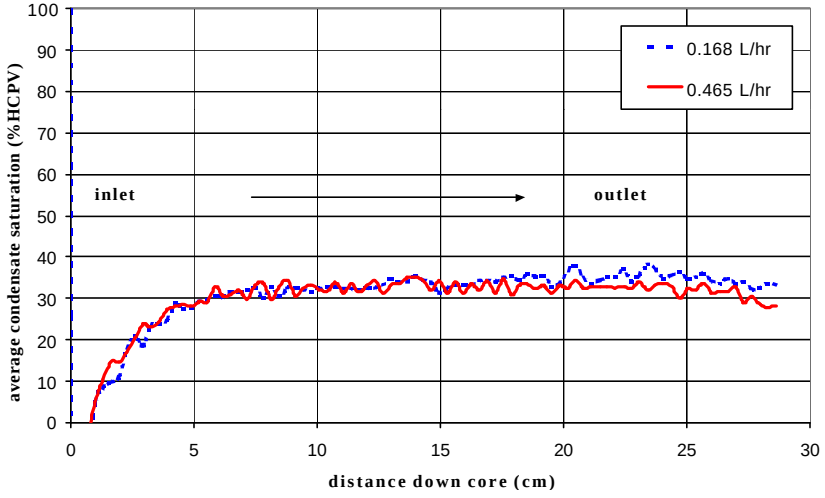

FIGURE 9: Condensate saturation profile: test hr_140

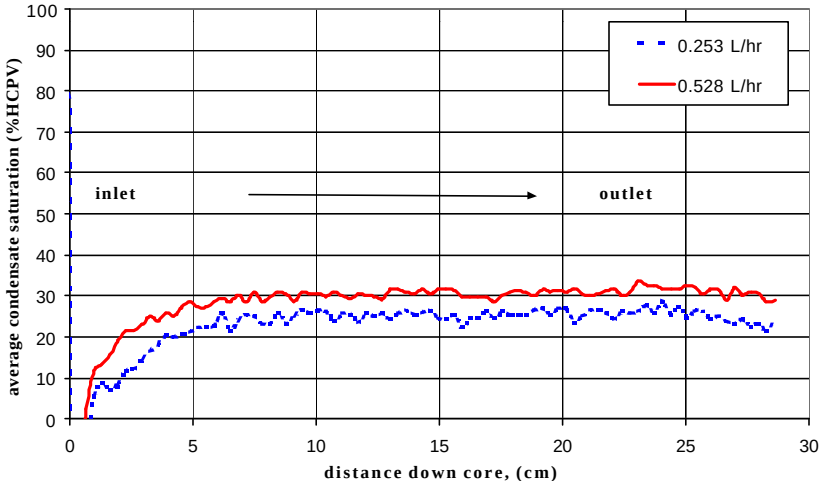

FIGURE 10: Condensate saturation profile: test hr_200

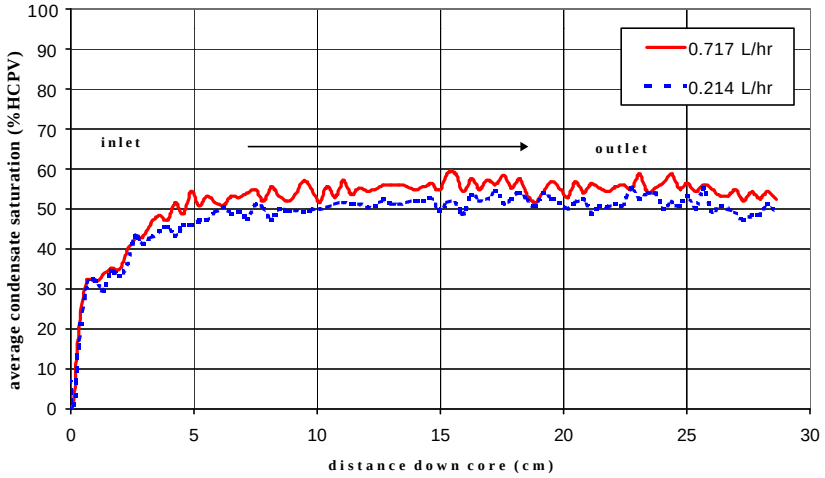

FIGURE 11: Condensate saturation profile: hr_150 (extended test)

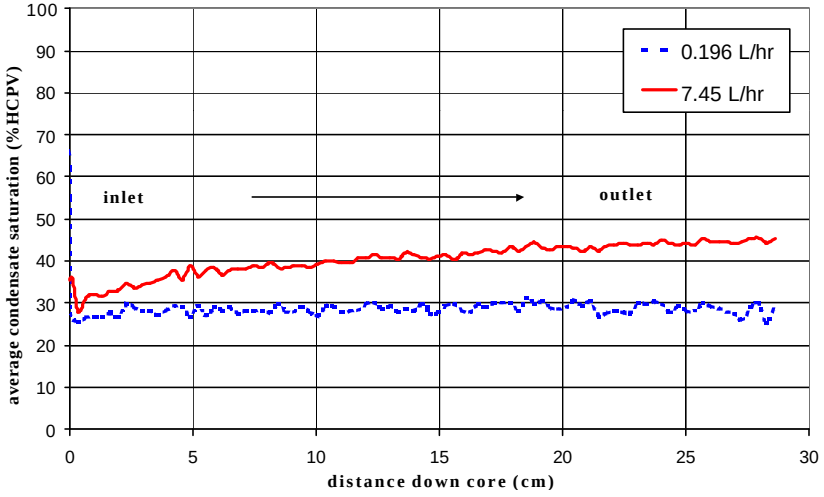

FIGURE 12: Relative Permeability Curves vs. Capillary Number